Elliptic Functions and Maximal Unitarity

Mads Søgaard[1] and Yang Zhang[2]

[1] *Niels Bohr International Academy and Discovery Center, Niels Bohr Institute, Blegdamsvej 17, DK-2100 Copenhagen, Denmark*

[2] *Institute for Theoretical Physics, ETH Zürich Wolfgang-Pauli-Straße 27, CH-8093 Zürich, Switzerland*

(Dated: June 3, 2015)

Scattering amplitudes at loop level can be reduced to a basis of linearly independent Feynman integrals. The integral coefficients are extracted from generalized unitarity cuts which define algebraic varieties. The topology of an algebraic variety characterizes the difficulty of applying maximal cuts. In this work, we analyze a novel class of integrals whose maximal cuts give rise to an algebraic variety with irrational irreducible components. As a phenomenologically relevant example we examine the two-loop planar double-box contribution with internal massive lines. We derive unique projectors for all four master integrals in terms of multivariate residues along with Weierstrass' elliptic functions. We also show how to generate the leading-topology part of otherwise infeasible integration-by-parts identities analytically from exact meromorphic differential forms.

arXiv:1412.5577v2 [hep-th] 2 Jun 2015

Modern perturbative scattering amplitudes in gauge theories such as QCD are calculated from general principles of analyticity and unitarity without inspecting Feynman diagrams. By virtue of analyticity, amplitudes are reconstructed from their singularity structure, while unitarity ensures that residues factorize onto simpler objects. Starting from complex internal momenta and three-point amplitudes whose form is entirely fixed by field theory arguments, all trees are generated recursively [1, 2] and then recycled for loops via unitarity cuts [3–6].

At the one-loop level, all amplitude contributions can be extracted directly from a small set of generalized unitarity cuts [7–9]. The computation is fully automated and has led to numerous precise predictions for collider physics. In the past few years, steps toward an analogous framework at two loops known as maximal unitarity have been reported; see refs. [10, 11] and subsequent generalizations [12–17]. Parallel developments at the level of the integrand can be found in e.g. refs. [21–24].

The increase of complexity at two loops requires a sophisticated approach. Previous works [10–20] lend credence to the belief of surmounting the problem by understanding the underlying algebraic and differential geometry of scattering amplitudes. The topology of the algebraic varieties associated with the maximal cuts examined so far has been that of degenerate elliptic and hyperelliptic curves of which the irreducible components are rationally parametrized Riemann spheres. The only algebraic curve at one loop is a conic section from the triangle diagram. In advanced problems such as maximal cuts in $D = 4-2\epsilon$ dimensions and massive internal particles, the irreducible components have nonzero genus, and it has been an open problem for years to deal with this class of integrals. In this paper, we present an analytic solution for genus-1 maximal cuts, based on Weierstrass' elliptic functions. Our method is used to predict new partial results for two-loop scattering with massive propagators.

The first step of multiloop amplitude calculations is to employ integrand-level reductions and integration-by-parts (IBP) relations to obtain a minimal basis of Feynman integrals $\{I_k\}$. The amplitude can thus be written

$$\mathcal{A}_n^{L\text{-loop}} = \sum_{k\in\text{Basis}} c_k I_k + \text{rational terms}\,, \tag{1}$$

and the c_ks are rational functions. The integrals are computed in dimensional regularization once and for all.

The coefficients are extracted by applying generalized unitarity cuts [7–9]. This operation is advantageous, because a loop-level amplitude may be broken into trees,

$$\sum_{k\in\text{Basis}} c_k I_k\big|_{\text{cut}} = \sum_{\text{states}} A^{\text{tree}}_{(1)} A^{\text{tree}}_{(2)} \cdots A^{\text{tree}}_{(m)}\,. \tag{2}$$

As factorization for general amplitude contributions is achievable only for complex-valued momenta, the refined unitarity cut prescription involves contour integrals,

$$\int_{\mathbb{R}} dz\,\delta(z-q) \longrightarrow \frac{1}{2\pi i}\oint_{C(q)} \frac{dz}{z-q}\,, \tag{3}$$

rather than delta functions. Here, $C(q)$ is a small circle centered at $q \in \mathbb{C}$. In the multidimensional case, the integration contour Γ is an n-torus, and the integrand is a differential form,

$$\omega(z) = \frac{h(z)dz_1\wedge\cdots\wedge dz_n}{f_1(z)\cdots f_n(z)}\,. \tag{4}$$

Let $\xi \in \mathbb{C}^n$ be an isolated zero of $f = (f_1,\ldots,f_n)$. The multivariate residue of ω at the pole ξ is said to be non-degenerate if $J(\xi) = \det_{i,j} \partial f_i/\partial z_j|_\xi \neq 0$. Explicitly,

$$(2\pi i)^n \,\text{Res}_{\{f_1,\ldots,f_n\},\xi}(\omega) = \oint_\Gamma \omega(z) = h(\xi)/J(\xi)\,. \tag{5}$$

For the degenerate case, see e.g. refs. [15–17].

To ensure consistency of maximal cuts, it is necessary to take appropriate linear combinations of residues to project out spurious terms which integrate to zero on the real slice [10]. The sources of spurious terms are parity-odd Levi-Civita contractions and parity-even IBP reductions. Accordingly, we demand that

$$I_1 = I_2 \implies I_1\big|_{\rm cut} = I_2\big|_{\rm cut} \,, \tag{6}$$

which imposes constraints on the weights. Resolving the constraints uniquely and deriving the master integral coefficients is the essential task in maximal unitarity.

The principal mathematical prerequisite for the remainder of this paper is the theory of elliptic curves; see e.g. refs. [25, 26]. We will study nondegenerate elliptic curves over the field of complex numbers, governed by the Weierstrass equation,

$$y^2 = 4x^3 - g_2 x - g_3 \,, \quad g_2^3 - 27 g_3^2 \neq 0 \,, \tag{7}$$

where g_2, g_3 are called the Weierstrass invariants. The elliptic curve (7) is topologically equivalent to a torus in $\mathbb{CP}^1$ that is naturally parametrized by Weierstrass' $\wp$-function and its first derivative. Indeed,

$$\wp'(z;g_2,g_3)^2 = 4\wp(z;g_2,g_3)^3 - g_2\wp(z;g_2,g_3) - g_3 \,, \tag{8}$$

is precisely of the form (7). The Weierstrass $\wp$-function is fixed once either g_2, g_3 or the half-periods ω_1, ω_2 are specified. For compactness we will just write $\wp(z)$. An essential property of the Weierstrass $\wp$-function is the addition law,

$$\wp(z) + \wp(w) + \wp(z+w) = \frac{1}{4}\left(\frac{\wp'(z) - \wp'(w)}{\wp(z) - \wp(w)}\right)^2 \,. \tag{9}$$

Below we will frequently encounter the function

$$\varphi(z,w) := \frac{1}{2}\frac{\wp'(z) - \wp'(w)}{\wp(z) - \wp(w)} \,. \tag{10}$$

It is expressible in terms of the Weierstrass ζ-function,

$$\varphi(z,w) = \zeta(z+w) - \zeta(z) - \zeta(w) \,. \tag{11}$$

Moreover, since $\zeta'(z) = -\wp(z)$,

$$\frac{d}{dz}\varphi(z,w) = \wp(z) - \wp(z+w) \,. \tag{12}$$

Finally, we introduce the Weierstrass σ-function. It is defined through a logarithmic derivative,

$$\frac{d}{dz}\log\sigma(z) = \zeta(z) \,, \tag{13}$$

and obeys the periodicity relation,

$$\sigma(z+2\omega_k) = -e^{2\eta_k(z+\omega_k)}\sigma(z) \,, \quad \eta_k := \zeta(\omega_k) \,. \tag{14}$$

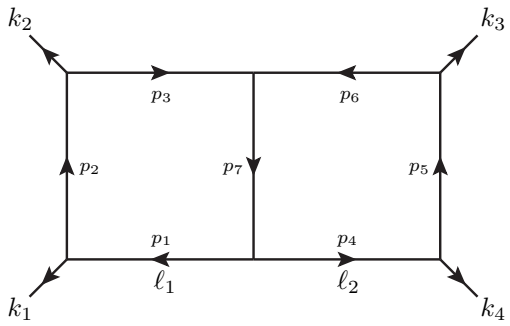

Figure 1. The planar double box.

Our primary example is the planar double-box integral with internal masses depicted in fig. 1. Without loss of the main features, we assume that external and internal lines are massless and massive, respectively. The outer-edge propagators carry mass m_1, while the particle in the middle rung has mass m_2. The corresponding Feynman integral is denoted I and can easily be read off.

It is convenient to parametrize loop-momenta ℓ_1, ℓ_2 as

$$\begin{aligned}
\ell_1^\mu &= \alpha_1 k_1^\mu + \alpha_2 k_2^\mu + \alpha_3 \frac{s}{2}\frac{\langle 1|\gamma^\mu|2]}{\langle 1\,4\rangle[4\,2]} + \alpha_4 \frac{s}{2}\frac{\langle 2|\gamma^\mu|1]}{\langle 2\,4\rangle[4\,1]} \,, \\
\ell_2^\mu &= \beta_1 k_3^\mu + \beta_2 k_4^\mu + \beta_3 \frac{s}{2}\frac{\langle 3|\gamma^\mu|4]}{\langle 3\,1\rangle[1\,4]} + \beta_4 \frac{s}{2}\frac{\langle 4|\gamma^\mu|3]}{\langle 4\,1\rangle[1\,3]} \,.
\end{aligned} \tag{15}$$

Simplifying the on-shell equations $p_1^2 = \cdots = p_6^2 = m_1^2$ yields $\alpha_1 = \beta_2 = 1$, $\alpha_2 = \beta_1 = 0$, $\alpha_3\alpha_4 = m_1^2 t(s+t)/s^3$ and $\beta_3\beta_4 = m_1^2 t(s+t)/s^3$. The remaining cut equation is quadratic in two variables, say, α_4 and β_4. The solution is of the form $\beta_4 = \big(A(\alpha_4) + \sqrt{\Delta(\alpha_4)}\big)/B(\alpha_4)$.

The nondegenerate multivariate residue associated with the hepta-cut of I easily follows from eq. (5),

$$I|_{7-\rm cut} \propto \oint \frac{d\alpha_4}{\sqrt{\Delta}} \,, \tag{16}$$

and the constant of proportionality is not important for the argument. The radicand Δ is a quartic polynomial,

$$\Delta = q_0(\alpha_4 - q)^4 + 6q_2(\alpha_4 - q)^2 + 4q_3(\alpha_4 - q) + q_4 \,, \tag{17}$$

for q_is which are rational functions of kinematic invariants. The constant $q = (m_2^2/(s-4m_1^2) - t/s)/2$ is designed to remove the cubic term.

Generically, the four roots of Δ are distinct, so $\eta^2 = \Delta$ defines an elliptic curve. The structure of the roots is complicated, but it is not necessary to solve for them explicitly. The elliptic curve is birationally equivalent to the Weierstrass form (7), with the Weierstrass invariants,

$$g_2 = (3q_2^2 + q_0 q_4)/q_0^2 \,, \quad g_3 = (q_0 q_2 q_4 - q_0 q_3^2 - q_2^3)/q_0^3 \,. \tag{18}$$

Via this birational transformation, the Weierstrass parametrization is found to be of the form,

$$\eta(z) = \sqrt{q_0}(\wp(z) - \wp(z+u)) \ , \quad \alpha_4(z) = \varphi(z,u) + q \ , \tag{19}$$

where u is the unique constant such that $\wp(u; g_2, g_3) = -q_2/q_0$ and $\wp'(u; g_2, g_3) = q_3/q_0$. Invoking eq. (12),

$$\frac{d}{dz}\alpha_4(z) = \frac{1}{\sqrt{q_0}}\eta(z) \implies I[1]\big|_{7-\text{cut}} \propto \oint dz \ . \tag{20}$$

Remarkably, all branch cuts are removed.

The half-periods of the torus associated with the elliptic curve are ω_1, ω_2. For real m_1, m_2, s_{12}, s_{14} we choose ω_1 to be purely imaginary (with negative imaginary part) and ω_2 to be real and positive. The fundamental cycles $\mathcal{A}$ and $\mathcal{B}$ are depicted in fig. 2. We trivially find

$$\oint_{\mathcal{A}} dz = 2\omega_1 \ , \quad \oint_{\mathcal{B}} dz = 2\omega_2 \ , \tag{21}$$

and the scalar integrand has no poles. Evaluated on the hepta-cut, a generic double-box numerator insertion is a polynomial in $\alpha_3(z), \alpha_4(z), \beta_3(z), \beta_4(z)$. Let us examine the $\alpha_4(z)$ insertion. The Weierstrass ζ-functions in eq. (11) can be integrated using eqs. (13) and (14), yielding

$$\begin{aligned}\oint_{\mathcal{A}} dz\alpha_4(z) &= 2q\omega_1 + \oint_{\mathcal{A}} dz \frac{1}{2}\frac{\wp'(z) - \wp'(u)}{\wp(z) - \wp(u)} \\ &= 2q\omega_1 + 2(u\eta_1 - \omega_1\zeta(u)) \ ,\end{aligned} \tag{22}$$

and likewise for the $\mathcal{B}$ cycle. The poles of $\alpha_4(z)$ on the z-torus are $z_1 := 0$ and $z_2 := -u$. By Laurent expansion,

$$\oint_{\mathcal{C}_1} dz\alpha_4(z) = -2\pi i \ , \quad \oint_{\mathcal{C}_2} dz\alpha_4(z) = +2\pi i \ , \tag{23}$$

where $\mathcal{C}_i$ is a cycle around z_i. These residues sum to zero by the Global Residue Theorem (GRT). The two poles of $\alpha_3(z)$, i.e. the two zeros of $\alpha_4(z)$, are located at $z_3 := z_1 + \omega_1 + \omega_2$ and $z_4 := z_2 + \omega_1 + \omega_2$. From the theory of elliptic functions, $\alpha_3(z) = \alpha_4(z - \omega_1 - \omega_2)$, so $\alpha_3(z)$ is just a shift of $\alpha_4(z)$. The shift leaves the fundamental cycle integrations invariant, and the residues are also $\pm 2\pi i$. This analysis extends seamlessly to linear insertions of $\beta_4(z)$ and $\beta_3(z)$. The two poles of $\beta_4(z)$ are denoted by z_5 and z_6, and a short calculation reveals that $z_6 = z_5 + z_2$ and $\beta_4(z) = \alpha_4(z - z_5)$. An expression for z_5 can be found from the Weierstrass parametrization of $\beta_4(z)$. Similarly, $\beta_3(z) = \alpha_4(z - z_7)$ and the poles are $z_7 = z_5 + \omega_1 + \omega_2$ and $z_8 = z_6 + \omega_1 + \omega_2$. We denote the set of numerator poles as $\mathcal{S} = \{z_1, \ldots, z_8\}$. In summary, there are two fundamental cycles $\mathcal{A}, \mathcal{B}$ and eight residue

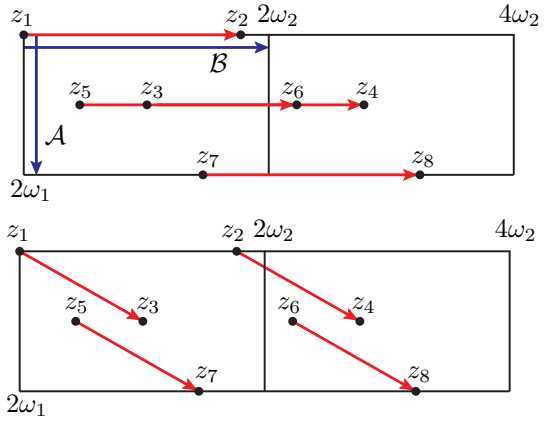

Figure 2. The distribution of and relations among the eight poles $(z_1, \ldots, z_8)$ in the underlying lattice of the elliptic functions. It can be seen that $z_{2i} = z_{2i-1} + z_2$ for $i = 1, 2, 3, 4$ and $z_{i+2} = z_i + \omega_1 + \omega_2$ for $i = 1, 2, 5, 6$.

cycles $\mathcal{C}_1, \ldots, \mathcal{C}_8$ on the torus. Schematically,

$$\begin{aligned}
&I_{0,0,0,0} \to (2\omega_1, 2\omega_2, 0, 0, 0, 0, 0, 0, 0, 0) \ , \\
&I_{0,1,0,0} \to (\mathcal{A}_{0,1,0,0}, \mathcal{B}_{0,1,0,0}, -2\pi i, 2\pi i, 0, 0, 0, 0, 0, 0) \ , \\
&I_{1,0,0,0} \to (\mathcal{A}_{1,0,0,0}, \mathcal{B}_{1,0,0,0}, 0, 0, -2\pi i, 2\pi i, 0, 0, 0, 0) \ , \\
&I_{0,0,0,1} \to (\mathcal{A}_{0,0,0,1}, \mathcal{B}_{0,0,0,1}, 0, 0, 0, 0, -2\pi i, 2\pi i, 0, 0) \ , \\
&I_{0,0,1,0} \to (\mathcal{A}_{0,0,1,0}, \mathcal{B}_{0,0,1,0}, 0, 0, 0, 0, 0, 0, -2\pi i, 2\pi i) \ ,
\end{aligned} \tag{24}$$

with $I_{a,b,c,d} := I[\alpha_3^a \alpha_4^b \beta_3^c \beta_4^d]$ and

$$\begin{aligned}
\mathcal{A}_{1,0,0,0} &= \cdots = \mathcal{A}_{0,0,0,1} = 2q\omega_1 + 2(u\eta_1 - \omega_1\zeta(u)) \ , \\
\mathcal{B}_{1,0,0,0} &= \cdots = \mathcal{B}_{0,0,0,1} = 2q\omega_2 + 2(u\eta_2 - \omega_2\zeta(u)) \ .
\end{aligned} \tag{25}$$

Note that $\eta_1\omega_2 - \eta_2\omega_1 = i\pi/2$. The surprisingly simple structure of the locus of poles is demonstrated in fig. 2.

The weights associated with the fundamental cycles and the eight residues are collected into a vector $\mathbf{\Omega}$,

$$\mathbf{\Omega} = (\Omega_{\mathcal{A}}, \Omega_{\mathcal{B}}, \Omega_1, \ldots, \Omega_8)^T \ . \tag{26}$$

We rewrite the remaining arbitrary one-dimensional integration contour in an overcomplete basis of the first homology group of the z-torus with poles excluded,

$$\begin{aligned}
I[\Phi] \longrightarrow \Omega_{\mathcal{A}} \oint_{\mathcal{A}} dz\Phi(z) + \Omega_{\mathcal{B}} \oint_{\mathcal{B}} dz\Phi(z) \\
+ 2\pi i \sum_{j=1}^{8} \Omega_j \, \text{Res}_{z=z_j} \Phi(z) \ ,
\end{aligned} \tag{27}$$

for a priori undetermined weights. The GRT implies that only seven of the residues are independent.

The double-box topology with internal masses m_1, m_2 has four master integrals, as can be verified from IBP identities generated by public computer codes. The masters are typically chosen to be of the form $I_{m,n} :=$

$I[(\ell_1\cdot k_4)^m(\ell_2\cdot k_1)^n]$. However, in practice it proves advantageous to adopt master integrals with chiral numerator insertions, for example,

$$(I_1,\ldots,I_4) = (I_{0,0,0,0},I_{0,1,0,0},I_{0,2,0,0},I_{0,1,1,0})\ . \tag{28}$$

Remarkably, there are five linearly independent constraints, leaving space for precisely four master integral projectors. The constraints can be cast as a matrix equation, $M\mathbf{\Omega}=0$, for a coefficient matrix M whose entries are simply integers,

$$M = \begin{pmatrix} 1 & -1 & 0 & 0 & 0 & 0 & 0 & 2 & 0 & -2 \\ 0 & 0 & 1 & 0 & 0 & -1 & 0 & 1 & -1 & 0 \\ 0 & 0 & 0 & 1 & 0 & -1 & 0 & 1 & 0 & -1 \\ 0 & 0 & 0 & 0 & 1 & -1 & 0 & 0 & -1 & 1 \\ 0 & 0 & 0 & 0 & 0 & 0 & 1 & -1 & -1 & 1 \end{pmatrix}\ . \tag{29}$$

The origin of four of the constraints is conjugation symmetry, i.e. Levi-Civita insertions which integrate to zero, whereas the last constraint reflects left-right symmetry of the double-box diagram. All constraints from IBP reduction are automatically satisfied. The rank-2 cut expressions in eq. (28) are of the form,

$$\begin{aligned} I_{0,2,0,0} &\to (\mathcal{A}_{0,2,0,0},\mathcal{B}_{0,2,0,0},-4\pi i q,4\pi i q,0,0,0,0,0,0)\ , \\ I_{0,1,1,0} &\to (\mathcal{A}_{0,1,1,0},\mathcal{B}_{0,1,1,0},r_+,r_-,0,0,0,0,-r_-,-r_+)\ , \end{aligned} \tag{30}$$

where $r_\pm$ are simple functions of external invariants and $\mathcal{A}_{0,2,0,0}$ and $\mathcal{B}_{0,2,0,0}$ are easy to derive using eq. (9). The analytic results for $\mathcal{A}_{0,1,1,0}$ and $\mathcal{B}_{0,1,1,0}$ are a bit more complicated.

Let $\mathcal{M}_i$ denote the projector which extracts I_i and normalizes its cut expression, respecting all constraints. The projectors can be written compactly as solutions to inhomogeneous matrix equations. Therefore we construct the 10×10 matrix,

$$F = \begin{pmatrix} M & G & I_1 & I_2 & I_3 & I_4 \end{pmatrix}^T\Big|_{\rm cut} \tag{31}$$

where transposition is with respect to the six blocks and $G=(0,0,0,0,0,0,0,0,0,1)$ implements the GRT. F has full rank and all four projectors are thus unique. Defining

$$\begin{pmatrix} \delta_1 & \delta_2 & \delta_3 & \delta_4 \end{pmatrix} = \begin{pmatrix} 0_{6\times 4} \\ 1_{4\times 4} \end{pmatrix}\ , \tag{32}$$

we arrive at the result, $\mathcal{M}_i = F^{-1}\delta_i$. Our final formula for the master integral coefficients is

$$\begin{aligned} c_i = \Omega^{(i)}_{\mathcal{A}} \oint_{\mathcal{A}} dz \prod_{k=1}^{6} A^{\rm tree}_{(k)}(z) + \Omega^{(i)}_{\mathcal{B}} \oint_{\mathcal{B}} dz \prod_{k=1}^{6} A^{\rm tree}_{(k)}(z) \\ + 2\pi i \sum_{j=1}^{8} \Omega^{(i)}_j \,{\rm Res}_{z=z_j} \prod_{k=1}^{6} A^{\rm tree}_{(k)}(z)\ . \end{aligned} \tag{33}$$

Note that the products of tree-level amplitudes are implicitly summed over all internal on-shell states in the theory.

An amazing property we developed is the relation between exact meromorphic differential forms and IBP identities. Let F be an elliptic function with poles inside $\mathcal{S}$, so $dF = f dz$ is an exact 1-form on $\mathbf{T}^2\setminus\mathcal{S}$. By Stokes' theorem, $\oint_{\mathcal{A},\mathcal{B}} dF = \oint_{\mathcal{C}_i} dF = 0$. So from eq. (27),

$$I[f] = 0 + \cdots \tag{34}$$

is an IBP identity. Here, $\cdots$ stands for integrals with fewer than seven propagators. Using the properties of Weierstrass' functions,

$$d(f_1(\alpha_4)\eta) = \frac{f_1'(\alpha_4)\Delta + \frac{1}{2}f_1(\alpha_4)\Delta'(\alpha_4)}{\sqrt{q_0}}dz\ , \tag{35}$$

$$d(f_2(\alpha_4)) = \frac{f_2'(\alpha_4)(B(\alpha_4)\beta_4 - A(\alpha_4))}{\sqrt{q_0}}dz\ , \tag{36}$$

for arbitrary polynomials f_1, f_2. Hence, we get the IBPs,

$$I[f_1'(\alpha_4)\Delta + \tfrac{1}{2}f_1(\alpha_4)\Delta'(\alpha_4)] = \cdots\ , \tag{37}$$

$$I[f_2'(\alpha_4)(B(\alpha_4)\beta_4 - A(\alpha_4))] = \cdots\ . \tag{38}$$

For example taking $f_2(\alpha_4)=\alpha_4$, the IBP

$$\begin{aligned} m_1^2t^2(s+t)I_{0,0,0,0} + 2s^4I_{0,2,0,1} + s^3tI_{0,2,0,0} + 2s^3tI_{0,1,0,1} \\ + s^2t(2m_1^2 - m_2^2 + t)I_{0,1,0,0} + 2m_1^2st^2I_{0,0,0,1} = \cdots \end{aligned} \tag{39}$$

is obtained. It is verified that eqs. (37) and (38) and similar relations with respect to the flip symmetry generate *all* IBP identities without doubled propagators for the massive double-box diagram. We expect that this relation between meromorphic exact forms and IBP identities would hold for other two-loop diagrams and lead to an extremely efficient algorithm for generating IBPs analytically.

We remark that one is not obliged to work in the Weierstrass standard form. Indeed, Weierstrass' elliptic functions are equivalent to the Jacobi elliptic functions. The fundamental parameter of our torus, $\tau = \omega_2/\omega_1$, is related to the elliptic modulus k via the j-invariant.

The calculations presented here yield a highly nontrivial addition to the body of evidence of the uniqueness conjecture of two-loop master integral projectors. In particular, our work continues to suggest a very intimate connection between the structure of maximal unitarity cuts and algebraic geometry and multivariate complex analysis. This paper gives rise to a host of new exciting directions in multiloop unitarity. The obvious extension is to formalize maximal cuts of double-box integrals in D dimensions. We expect this can be done by analytic continuation. Our method presumably applies directly to the purely massless double-box contribution to ten-gluon scattering [11]. It would be very interesting to understand the structure of maximal cuts which define hyperelliptic curves, for example from the nonplanar double box, and more generally, topologically nontrivial

surfaces. We are also intrigued by investigating the relation between maximal cuts and evaluation of master integrals. These problems provide avenues for discovering further relations between scattering amplitudes and areas of mathematics.

Acknowledgments: We have benefited from discussions with N. Beisert, N.E.J. Bjerrum-Bohr, S. Caron-Huot, P.H. Damgaard, H. Frellesvig, R. Huang, H. Ita, H. Johansson, D.A. Kosower and K.J. Larsen. MS and YZ are grateful to the Institute for Theoretical Physics at ETH Zürich and the HKUST Jockey Club Institute, respectively, for hospitality during phases of this project. The research leading to these results has received funding from the European Research Council under the European Union's Seventh Framework Programme (FP/2007-2013) / ERC Grant Agreement no. 615203. The work is partially supported by the Swiss National Science Foundation through the NCCR SwissMAP.

[1] R. Britto, F. Cachazo and B. Feng, Nucl. Phys. B **715**, 499 (2005) [hep-th/0412308].
[2] R. Britto, F. Cachazo, B. Feng and E. Witten, Phys. Rev. Lett. **94**, 181602 (2005) [hep-th/0501052].
[3] Z. Bern, L. J. Dixon, D. C. Dunbar and D. A. Kosower, Nucl. Phys. B **425**, 217 (1994) [hep-ph/9403226].
[4] Z. Bern, L. J. Dixon, D. C. Dunbar and D. A. Kosower, Nucl. Phys. B **435**, 59 (1995) [hep-ph/9409265].
[5] Z. Bern, L. J. Dixon and D. A. Kosower, Nucl. Phys. B **513**, 3 (1998) [hep-ph/9708239].
[6] Z. Bern, L. J. Dixon and D. A. Kosower, JHEP **0001**, 027 (2000) [hep-ph/0001001].
[7] R. Britto, F. Cachazo and B. Feng, Nucl. Phys. B **725**, 275 (2005) [hep-th/0412103].
[8] D. Forde, Phys. Rev. D **75**, 125019 (2007) [arXiv:0704.1835 [hep-ph]].
[9] S. D. Badger, JHEP **0901**, 049 (2009) [arXiv:0806.4600 [hep-ph]].
[10] D. A. Kosower and K. J. Larsen, Phys. Rev. D **85**, 045017 (2012) [arXiv:1108.1180 [hep-th]].
[11] S. Caron-Huot and K. J. Larsen, JHEP **1210**, 026 (2012) [arXiv:1205.0801 [hep-ph]].
[12] H. Johansson, D. A. Kosower and K. J. Larsen, Phys. Rev. D **87**, 025030 (2013) [arXiv:1208.1754 [hep-th]].
[13] H. Johansson, D. A. Kosower and K. J. Larsen, Phys. Rev. D **89**, 125010 (2014) [arXiv:1308.4632 [hep-th]].
[14] M. Sogaard, JHEP **1309**, 116 (2013) [arXiv:1306.1496 [hep-th]].
[15] M. Sogaard and Y. Zhang, JHEP **1312**, 008 (2013) [arXiv:1310.6006 [hep-th]].
[16] M. Sogaard and Y. Zhang, JHEP **1407**, 112 (2014) [arXiv:1403.2463 [hep-th]].
[17] M. Sogaard and Y. Zhang, JHEP **1412**, 006 (2014) arXiv:1406.5044 [hep-th].
[18] R. Huang and Y. Zhang, JHEP **1304**, 080 (2013) [arXiv:1302.1023 [hep-ph]].
[19] J. D. Hauenstein, R. Huang, D. Mehta and Y. Zhang, arXiv:1408.3355 [hep-th].
[20] Y. Zhang, arXiv:1408.4004 [hep-th].
[21] S. Badger, H. Frellesvig and Y. Zhang, JHEP **1204**, 055 (2012) [arXiv:1202.2019 [hep-ph]].
[22] Y. Zhang, JHEP **1209**, 042 (2012) [arXiv:1205.5707 [hep-ph]].
[23] S. Badger, H. Frellesvig and Y. Zhang, JHEP **1208**, 065 (2012) [arXiv:1207.2976 [hep-ph]].
[24] S. Badger, H. Frellesvig and Y. Zhang, JHEP **1312**, 045 (2013) [arXiv:1310.1051 [hep-ph]].
[25] J. H. Silverman, "The Arithmetic of Elliptic Curves". Springer, 2010.
[26] E. T. Whittaker and G. N. Watson, "A Course of Modern Analysis". Cambridge University Press, 1996.